Advanced Ceramics Progress

Fabrication of Graphene Oxide Thin Films on Transparent Substrate via a Low-Voltage Electrodeposion Technique

Z. Abadi, P. Sangpour*, F. Tajabadi

Department of Nanotechnology and Advanced Materials, Materials and Energy Research Center, Karaj, Iran

ABSTRACT

Graphene oxide (GO) thin films were simply deposited on fluorine doped tin oxide (FTO) substrate via a low-voltage electrodeposition. The GO and GO thin films were characterized by Zeta Potential, X-ray diffraction, Ultraviolet-Visible spectroscopy, atomic force microscopy, Fourier transform infrared spectroscopy, field emission scanning electron microscopy and energy dispersive X-ray spectroscopy. The results confirm existence of multi-layered graphene oxide. UV-vis spectra exhibit GO thin films possess 60-80% transmittance in the visible region. Calculating calculating optical band gap from UV-vis spectra either for GO solution and GO thin film suggests a simultaneous reduction occurred during deposition.

1. INTRODUCTION

Graphene, a planar structure and hexagonal network of sp^2 bonded carbon atoms, has distinctive electrical and mechanical properties which include extremely high side ratios, large surface area, high carrier mobility, high Young's modulus, and excellent thermal and electrical conductivities [1]. Graphene oxide (GO) can be considered as one or a few graphene sheets which is functionalized by a range of oxygenated groups as a result of the graphite powder reaction with strong oxidizing agents such as a mixture of concentrated sulfuric acid and potassium permanganate [1]. More specifically, epoxied and hydroxyl groups are present on its basal planes while the edges are decorated with carboxylic acids and various other groups depending on the pH of suspension [2]. A schematic representation of a GO sheet and its functional groups is shown in Figure 1. The harsh chemical reactions introduce different kinds of defects to the graphene sheets and this leads to degradation of some important properties such as carrier mobility. On the other hand, the presence of these oxygenated groups makes GO soluble in water and some organic solvents [3], [4]. Its solution processability makes GO a promising candidate for a wide-variety of applications like graphene-based electronics devices [5], biosensors [6] and electrochemical sensors [7].These unique properties inspire many researchers to make an attempt to develop efficient graphene deposition techniques. Various methods such as spin coating [8], Langmuir−Blodgett Assembly [9], and dip coating [10] are suggested to prepare a graphene-based thin film. But these methods are limited by the surface area of deposited films. In this regard electrodeposition method can be considered as a simple and large scale deposition method for GO thin film fabrication. In this paper, we report the fabrication and characterization processes of a GO thin film via a low voltage electrodeposition (ED) route. It is important to consider that the electrochemical reduction of some functional groups takes place during ED and it is more intensive at higher voltages [11]. Additionally, the higher voltage may cause gas evolution and water decomposition [12] that can destroy the deposited GO film. In contrast, by applying lower voltage for ED, GO reduction, water decomposition and gas evolution are significantly avoidable. Therefore, the deposition conditions can be precisely controlled and an excellent adhesion to the substrate obtained as well.

2. EXPERIMENTAL

Graphite oxide was synthesized from natural graphite powder by the modified Hummer's method [9]. Briefly,

*Corresponding Author's Email: sangpour@merc.ac.ir (P. Sangpour)

500mg graphite (30μm, Powder, Merck) was mixed with 500mg $NaNO_3$ and 23ml concentrated H_2SO_4. Then 3g $KMnO_4$ was added to the mixture placed in an ice bath. Thereafter,the mixture was stirred for 24h in the 35°C oil bath. Subsequently, 100ml deionized (DI) water and 3ml H_2O_2 added drop-wise to the mixture. In order to remove undesirable ions, the obtained GO slurry was washed with HCl (10 vol%) and DI water untill a neutral pH obtained.
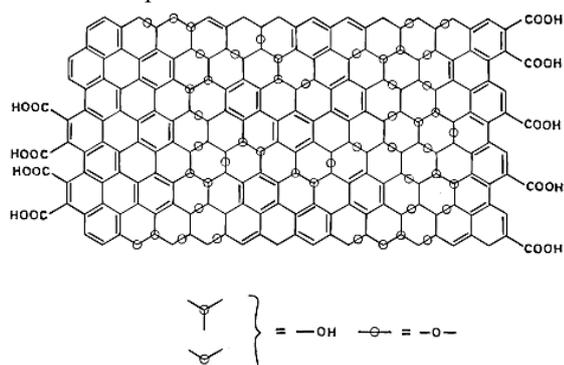
Figure 1. Structural model of GO proposed by LERF-Klinowski [27].

The as-synthesized graphite oxide was dispersed in deionized water under ultrasonication for 60 mins to prepare 2mg/mL graphene oxide solution. In order to get the GO thin film, the fluorine-doped tin oxide (FTO) glass substrate was put into GO suspension and the GO thin film deposition was done by using a three electrode system in a standard electrochemical cell. In this system, FTO-coated glasses were used as working and counter electrodes and Ag/AgCl as a reference electrode. Deposition was done under -1.5V potential for 100s whereas the distance between two electrodes was set 1 cm. The as-deposited film was washed thoroughly with DI water and then dried in air. Prior to using FTO-coated substrates, they were rinsed by using appropriate detergent, DI water and ethanol in an ultrasonic bath. Figure 2a. and 2b. show a schematic representation for ED cell and ED electrical current-time (I-t) plot, respectively.
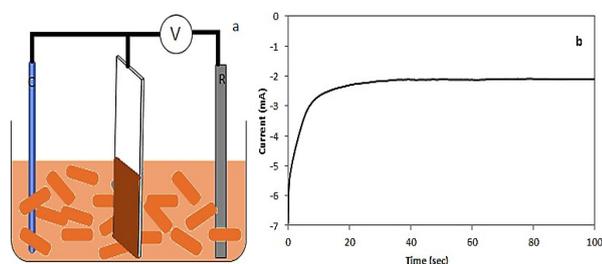
Figure 2. a) Schematic representation of ED in a standard three-electrode cell, counter and reference electrodes are indicated with C and R, respectively; b) Resultant electric current as a function of deposition time (measured by Autolab) during potentiostat ED in -1.5V.

3. CHARACTERIZATIONS

X-ray diffraction (Philips PW 3710 x-ray Diffractometer with Cu Kα radiation) was utilized to confirm GO formation and interlayer distance was obtained by Bragg's equation ($n\lambda=2dsin(\theta)$) where λ is wavelength of X-ray, θ is scattering angle and d corresponds to interlayer distance. The Fourier transform infrared spectroscopy (FTIR) spectrum was recorded in the range 4000–500 cm^{-1} by using the Perkin Elmer, Spectrum RXI. Zeta potential (ζ) measurements were carried out by Malvern Zeta sizer 3000 HSA to evaluate the stability of GO suspension used for electrodeposition. In order to study the morphology of thin films, field emission scanning electron microscopy (FESEM) images was taken by Hitachi S4160 and FESEM/EDX was done by Mira 3-XMU. To investigate individual GO sheet properties including lateral size and thickness, atomic force microscopy (AFM) images were obtained by Veeco Autoprobe CP-Research with asilicon tip of 10 nm radius in non-contact mode. Film thickness was measured by Profilometer. Finally, Ultraviolet-visible spectroscopy (PerkinElemer) was used to evaluate transmittance of thin film and the optical band gap.

4. RESULTS AND DISCUSSION

Figure 3. shows the X-ray diffraction pattern (XRD) of a dried GO sample.The sharp diffraction peak was observed at 2θ =10.5° with an interlayer distance of 8.40 Å corresponds to (001) plane (d001) for the AB-stacked GOs [13]. The GO interlayer distance is proportional to the amount of oxygen functional groups formed on basal planes [3].The small peak appeared at 2θ=21° corresponds to (002) plane of GO [13]. The XRD exhibit no extra peak indicating prepared GO contains no impurity.
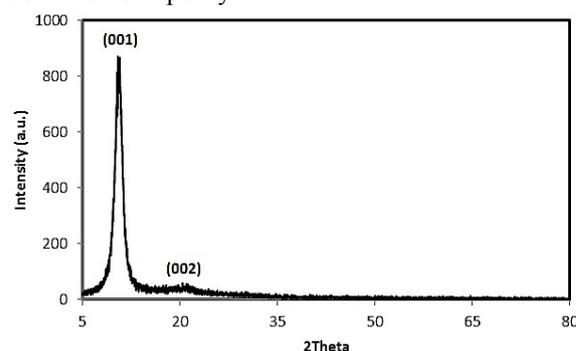
Figure 3. XRD pattern of dried GO.

Hun Hah [14] showed that there is a correlation between (001) peak and the number of stacked GO sheets. According to Hun Huh [14] and N. Faal [28], the average number of layers in the lamellar structure of GO can be computed from the position of (001) reflection by applying equation (1):

$$L_{001} = \frac{0.9}{B_{001}\cos\theta} \tag{1}$$

Where the stacking height (L_{001}) of the crystallite is determined by using the equation (1) where λ is the wavelength of X-ray used, B_{001} is the full width at half maximum of the (001) peak and θ is the corresponding scattering angles. If each parallel layer consists of N layers, L_{001} for aparallel layer group is obtained by:

$$L_{001} = (N-1)d_{001} \tag{2}$$

The (001) profile was fitted to obtain the number of layers of graphene oxide. So, according to above equations, we have calculated the average number of restacked layers of graphene oxide, and it was found to be nine sheets. The profile and the number of layers are summarized in Table 1.

Table 1. D spacing, number of layers and crystallite size from the X-ray diffraction pattern of GO sample.

Peak pos. [°2Th]	Crystallite size [A]	d spacing [A]	number of layer
10.525	65	8.39875	9

Fourier transform infrared (FTIR) spectrum of the GO is shown in Figure 4. The IR frequency associated with different functional groups and related bonds is marked in the picture. The existence of these oxygen-containing groups reveals that the graphite has successfully been oxidized to graphene oxide. Since GO is highly hygroscopic, a broad peak observed at 3415 cm^{-1} is caused by the stretching vibration of -OH groups of adsorbed water molecules. The absorption peak occurring at 1743 cm^{-1} originates from the stretching vibration of C=O of carboxylic and carbonyl groups placed at the edges of GO sheet and the absorption peaks at 1229 cm^{-1} is caused by the C-O-C bonds of epoxy in GO [15].The small peaks observed at 1420 cm^{-1} and 1050 cm^{-1} can be attributed to C-OH deformation and C-O stretching bonds, respectively. Finally, the peak appeared at 1628 cm^{-1} is assigned to C=C ring from unoxidized sp^2 CC bond [16].
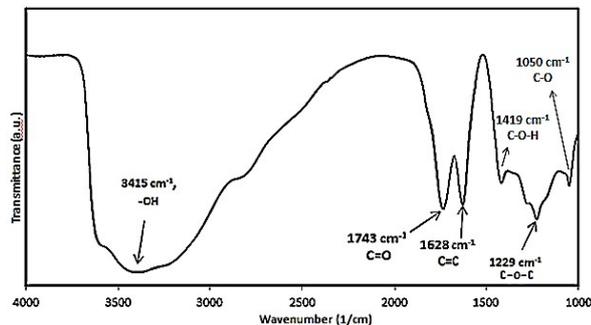
Figure 4. FTIR spectrum of dried GO.

Multi-layered graphene oxide was confirmed by noncontact atomic force microscopy (AFM). To obtain AFM images of GO sheets, electrodeposited GO films

were used. In accordance with previous reports [17], the thickness of monolayer GO should be about 1 nm which is larger than an individual sheet of graphene (about 0.34 nm). This is due to the presence of hydroxyl and epoxide groups, structural defects, and adsorbed water molecules on GO sheets [18]. As can be seen in thickness profile, AFM images revealed the mean thickness of GOs are approximately 10 nm. These results are interpreted to correspond to 10 stacked layers with lateral dimensions of several hundred nanometers. This result is in good agreement with XRD obtained stacked sheets.
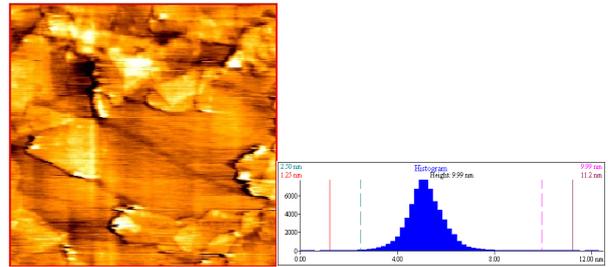
Figure 5. AFM image obtained from electrodeposited GO thin film and its height profile.

The zeta potential (ζ) is an important factor for characterizing the stability of colloidal dispersions and provides a measure of the magnitude and sign of the effective surface charge associated with the double layer around colloidal particles[4]. The zeta potential was taken as an average over twenty four measurements at pH=5. The Zeta potential of GO solution is evaluated to be -48.5mV, which is in a good agreement with those reported earlier[4]. The resultant value for ζ indicates a high colloidal stability for dispersed GO in water at this particular pH. Furthermore, this suggests that the stability of the GO dispersions is a consequence of the negatively charged functional groups on the GO sheets as shown in Figure 1. The presence of these oxygen containing functional groups makes GO highly hydrophilic.

The FESEM images of GO-covered FTOs are presented in Figure 6. with different magnifications. It is obviously seen that FTO substrate are fully covered with a uniform 200 nm GO film. Since the thickness of the film is so small, the F-doped SnO_2 grains from FTO substrate are visible in images. EDX spectroscopy, shown in Figure 6d. was performed on the GO-coated FTO substrate to examine the elemental composition. According to Figure 6d. the existence of carbon is confirmed in combination with some other elements including Sn, Si, O and F originated from FTO coated glass. Some extent of oxygen atoms comes from functional groups of graphene oxide sheets.

Figure 7a. shows the ultraviolet-visible spectrum of aqueous graphene oxide suspension. It has an absorption peak at 230 nm which is attributed to π - $\pi*$ transition of the aromatic C=C ring. This suggests that GO samples

possess an ordered graphitic structure [19]. According to previous reports, the π-π* plasmon peak depends on two different conjugate effect: one is related to nanometer scale sp^2 clusters, and the other arises from linking chromophore units such as C=C, C=O and C–O bonds [20]. Another characteristic feature is a shoulder at 300 nm corresponding to n-π* plasmon of C=O [20]. An optical band gap of GO can be calculated by Tauc equation [21]:

$$(\alpha h \vartheta)^{1/n} = A(h\vartheta - E_g) \qquad (3)$$
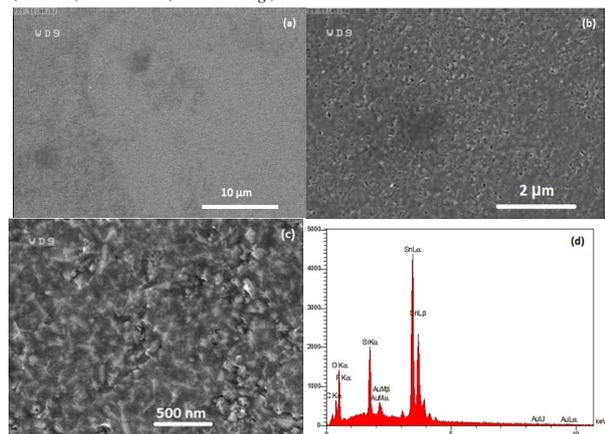
Figure 6. FESEM images of GO coated FTO substrates with different magnifications, a)a smooth surface of uniformly covered GO film ; b,c) GO film on FTO, the observed grains are related to FTO substrate ; d) Energy Dispersive X-ray Spectrum.

Where α is optical absorbance, hv is the photon energy and E_g is the optical band gap [22]. Depending on the type of optical transition caused by the photon absorption, n can have different values of ½ and 2 for direct and indirect transitions, respectivrly. In the case of graphene oxide, according to previous reports [19] n was chosen for the best fit to ½ indicating a direct-allowed transition. Because the amorphous GO sheet has a heterogeneous oxidation level, it can not exhibit sharp adsorption edges in the Tauc plot [19]. As can be seen in Figure 7b. using a linear extrapolation on Tauc plot leads to an approximate direct band gap of 3.5 eV for the dispersed GO in water. This result is in a good agreement with several other reports [19]. It is worth mentioning that band gap of GO directly depends on the ratio of carbon bonds to oxygenated functional groups and their different arrangements [23].

Optical transmittance spectrum of deposited GO thin film is shown in Figure 8a. As can be seen, GO thin film displays60-80% transmittance in the visible region. It is important to mention by applying lesser deposition time the thickness of the film and its transmittance become precisely controllable.

To compare the optical band gap of GO before and after deposition process, Eg of GO thin film was calculated by Tauc equation, too. According to Tauc plot in Figure

7b. and Figure 8b. optical band gap for GO thin film were determined to be about 2.2 eV which is considerably lower than E_g of GO solution. These results indicate that GO is simultaneously reduced during deposition.
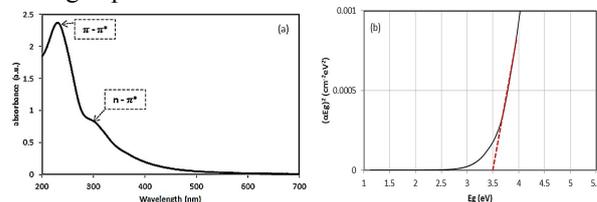
Figure 7. a) UV-Vis spectrum of GO solution in water; b) related Tauc plot.
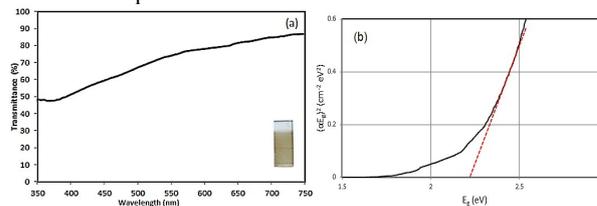
Figure 8. a) Optical transmittance spectrum of deposited GO thin; Inset: GO film onto FTO; b) Tauc plot for deposited GO film.

Although graphene is known as a zero-gap material, the presences of oxygenated groups with GO can induce a band gap [18]. Evolution of the electronic properties reveals that as-synthesized GO undergoes in sulator to semiconductor to semi-metal transitions [24] and some of its key features, including band gap, can be tuned by controlling its oxidation or reduction degree. In other words, since the electrical properties of GO and rGO is strongly correlated with sp^2 and sp3hybridization, restoring sp^2 bonding by various reduction methods [25] provides a strict control over its electronic properties. The possibility of band gap engineering in GO is of great interest in research communities for its implementation in functional photonic, nano electronic and sensing devices [24]. It is worth mentioning that in some applications it is critical to possess a uniform GO thin film on transparent substrate. Jun Liu et al [10] utilized spincoated graphene oxide nano ribbon film onto tin-doped in dium oxide (ITO) substrate as an hole extraction layer to enhance the efficiency and stability of polymer solar cells [10]. Bo Ram Lee [26] reported using GO film as an interlayer between the ITO and the active polymer in polymer light-emitting diodes. This interlayer enhanced device performance and its efficiency levels by maximizing hole–electron recombination within the emissive layer.

5. CONCLUSION

Graphene oxide thin films were successfully fabricated through an electro deposition method.The results show uniform fully covered substrate with 60-80% transparency. Expressing lower band gap for GO thin

film suggests that electrochemical reduction occurred during deposition. To sum up, we present a precisely controllable GO deposition on transparent substrates which provides a scalable uniform coating with an excellent adhesion. Thus, we believe that such a simple method is a cost effective candidate for various applications.

6. ACKNOWLEDGEMENT

REFERENCES

1. Dreyer, D.r., Park, S., Bielawski, C.W. and Ruoff, R.S., "The chemistry of graphene oxide", *Chemical Society Reviews,* Vol. 39, (2010), 228-240.

2. Dreyer, D.R., Todd, A.D. and Bielawski, C.W., "Harnessing the chemistry of graphene oxide", *Chemical Society Reviews,* Vol. 43, (2014), 5288-5301.

3. Park, S., An, J., Jung, I., Piner, R.D., An, S.J., Li, X., Velamakanni, A. and Ruoff R.S., "Colloidal Suspensions of Highly Reduced Graphene Oxide in a Wide Variety of Organic Solvents", *Nano Letters,* Vol. 9, (2009), 1593–1597.

4. Muszynski, R., Seger, B. and Kamat, P.V., "Decorating Graphene Sheets with Gold Nanoparticles", *The Journal of Physical Chemistry Letters,* Vol. 112, (2008), 5263–5266.

5. Standley, B., Mendez, A., Schmidgall, E. and Bockrath, M., "Graphene−Graphite Oxide Field-Effect Transistors", *Nano Letters,* Vol. 12, (2012), 1165-1169.

6. Kuila, T., Bose, S., Khanra, P., Mishra A.K., Kim N.H. and Lee, J.H., "Recent advances in graphene-based biosensors. Biosens Bioelectron", *Biosensors and Bioelectronics,* Vol. 26, (2011), 4637-4648.

7. Pumera, M., Ambrosi, A., Bonanni, A., Chng, E.L.K. and Poh, H.L., "Graphene for electrochemical sensing and biosensing", *TrAC Trends in Analytical Chemistry,* Vol. 29, (2010), 954–965.

8. Selopal G.S., Milan, R., Ortolani, L., Morandi, V., Rizzoli, R., Sberveglieri, G., Veronese, G.P., Vomierob, A. and Concina, I., "Graphene as transparent front contact for dye sensitized solar cells", *Solar Energy Materials and Solar Cells,* Vol. 135, (2015), 99–105.

9. Cote, L.J., Kim, F. and Huang J., "Langmuir−Blodgett Assembly of Graphite Oxide Single Layers", *Jornal of American Chemical Society,* Vol. 131, (2009), 1043–1049.

10. Becerril, H.A., Mao, J., Liu, Z., Stoltenberg, R.M., Bao, Z. and Chen Y., "Evaluation of Solution-Processed Reduced Graphene Oxide Films as Transparent Conductors", *American Chemical Society Nano,* Vol. 2, (2008), 463–470.

11. Ambrosi, A. and Pumera M., "Precise tuning of surface composition and electron-transfer properties of graphene oxide films through electroreduction", *Chemistry - A European Journal,* Vol. 19, (2013), 4748-4753.

12. Diba, M., García-Gallastegui, A., Taylor, R.N.K., Pishbin, F., Ryan, M.P., Shaffer, M.S.P. and Boccaccini A.R., "Quantitative evaluation of electrophoretic deposition kinetics of graphene oxide", *Carbon,* Vol. 67, (2014), 656–661.

13. Shi-Jia, M., Yu-Chang, S., Li-Hua, X., Si-Dong, L., Te., H. and Hong-Bo, T., "X-Ray Diffraction Pattern of Graphite Oxide", *Chinese Physical Letters,* Vol. 30, No. 9, (2013).

14. Huh S.H., "X-ray diffraction of multi-layer graphenes: Instant measurement and determination of the number of layers", *Carbon,* Vol. 78, (2014), 617–621.

15. Jabari-Seresht, R., Jahanshahi, M., Rashidi, A.M. and Ghoreyshi A.A., "Synthesis and Characterization of Thermally-Reduced Graphene", *Iranica Journal of Energy & Environment,* Vol. 4, (2013), 53-59.

16. Marcano, D.C., Kosynkin, D.V., Berlin, J.M., , Sinitskii, A., Sun, Z., Slesarev, A., Alemany, L.B., Lu, W. and Tour, J.M., "Improved Synthesis of Graphene Oxide", *American Chemical Society Nano,* Vol. 4 ,(2010), 4806–4814.

17. Yu, J.J. and Wu, S., "Single-pass kelvin force microscopy and dC/dZ imaging: applications for graphene-related nanomaterials", *Journal of Physics: Conference Series*, Vol. 483, (2014), 1-6.

18. Mkhoyan, K.A., Contryman, A.W., Silcox, J., Stewart, D.A., Eda, G., Mattevi, C., Miller, S. and Chhowalla, M., "Atomic and Electronic Structure of Graphene-Oxide", *Nano Letters,* Vol. 9, (2009), 1058–1063.

19. Hsu, H.C., Shown, I., Wei, H.Y., Chang, Y.C., Du, H.Y., Lin, Y.G., Tseng, C.A., Wang, C.H., Chen, L.C., Lin, Y.C. and Chen, K.H., "Graphene oxide as a promising photocatalyst for CO2 to methanol conversion", *Nanoscale,* Vol. 5, (2013), 262-268.

20. Lai, Q., Zhu, S., Luo, X., Zou, M. and Huang, S., "Ultraviolet-visible spectroscopy of graphene oxides", *American Institute of Physics Advances,* Vol. 2, (2012).

21. Tauc, J., Grigorovici, R. and Vancu, A., "Optical Properties and Electronic Structure of Amorphous Germanium", *physica status solidi (b),* Vol. 15, No. 2, (1966), 627–637.

22. Tsuchiya, T., Terabe, K. and Aono, M., "In Situ and Non-Volatile Bandgap Tuning of Multilayer Graphene Oxide in an All-Solid-State Electric Double-Layer Transistor", *Advanced Materials,* Vol. 26, (2014), 1087-1091.

23. Shang, J., Ma, L., Li, J., Ai, W., Yu, T. and Gurzadyan, G.G., "The Origin of Fluorescence from Graphene Oxide", *Scientific Reports,* Vol. 2, (2012), 1-8.

24. Eda, G., Mattevi, C., Yamaguchi, H., Kim, H. and Chhowalla, M., "Insulator to Semimetal Transition in Graphene Oxide *The Journal of Physical Chemistry C,* Vol. 113, (2009), 15768–15771.

25. Chua, C.K. and Pumera, M., "Chemical reduction of graphene oxide: a synthetic chemistry viewpoint", *Chemical Society Reviews,* Vol. 43, (2014), 291-312.

26. Lee, B.R., Kim, J.W., Kang, D., Lee, D.W., Ko, S.J., Lee, H.J., Lee, C.L., Kim, J.Y., Shin, H.S. and Song, M.H., "Highly Efficient Polymer Light-Emitting Diodes Using Graphene Oxide as a Hole Transport Layer", *American Chemical Society Nano,* Vol. 6, (2012), 2984–2991.

27. Lerf, A., He, H., Forster, M. and Klinowski, J., "Structure of Graphite Oxide Revisited", *The Journal of Physical Chemistry B,* Vol. 102, (1998), 4477–4482.

28. Faal Nazari, N.S., Saffaria, M.M. and Bazyar E., "X-ray Diffraction: A Multifunctional method for Graphene type structure characterization", Proceedings of the 5th International Conference on Nanostructures, (2014), Kish-Iran.